Z-99

# CONVERTED WAVES COMMON AZIMUTH MIGRATION

DANIEL A. ROSALES* AND BIONDO BIONDI
*Department of Geophysics, Stanford University, Stanford, CA 94305, USA*

## 1 Summary

Extending existing single mode PP 3-D prestack wavefield-based migration algorithms is possible for converted mode PS. The process just require a careful implementation of the appropriate velocity field for the downgoing and upcoming wavepaths. Understanding this process is of crucial importance in order to combine different but yet complementary data sets for exploration and characterization of oil reservoir. Numerical examples show the differences on processing both single and converted mode particularly with common-azimuth migration.

## 2 Introduction

Multicomponent seismic has several applications for oil exploration and reservoir characterization. Multicomponent seismic is different than conventional seismic; therefore, the development of new techniques to process converted waves data is important. Prominent progress has been done in many areas of converted waves seismic processing; as for example, stacking, DMO, migration and velocity analysis (Tessmer and Behle, 1988; Iverson et al., 1989; Huub Den Rooijen, 1991; Alfaraj, 1992; Harrison and Stewart, 1993). However, more advanced techniques for single mode PP seismic still does not have a counterpart for converted waves seismic.

Common azimuth migration is an efficient and robust technique for obtaining accurate single mode PP subsurface 3-D seismic images. This technique takes advantage of the reduced dimensionality of the computational domain. It assumes that the data have zero cross-line offset; that is, all the traces in the data share the same azimuth (Biondi and Palacharla, 1996). Due to the growing number of 3-D multicomponent seismic data sets, in areas where an accurate processing is required to obtain better subsurface images and/or estimate rock properties, wavefield-based continuation methods for converted mode data are of great importance and are totally needed in the oil industry today.

Converted waves common azimuth migration is very similar to the original common azimuth migration. It uses different propagation velocities for different wavefields. We compare the differences between single mode and converted mode common azimuth migration, and its possible implications for rock property estimation.

## 3 Converted waves common azimuth migration

The point-scatter geometry is a good starting point to discuss converted waves prestack common azimuth migration. The equation for the travel time is the sum of a downgoing travel path with P velocity ($v_p$) and an upcoming travel path with S velocity ($v_s$) as:

$$t = \frac{\sqrt{z^2 + \|\mathbf{s} - \mathbf{x}\|^2}}{v_p} + \frac{\sqrt{z^2 + \|\mathbf{g} - \mathbf{x}\|^2}}{v_s}, \qquad (1)$$

where **s** and **g** represents the source and receiver vector locations and **x** is the point-scatter subsurface position.

Common azimuth migration is a wavefield-based downward continuation algorithm. The algorithm is based on a recursive solution of the one-way wave equation (Claerbout, 1985). The basic continuation step used to compute the wavefield at depth $z+\Delta z$ from the wavefield at depth $z$ can be expressed in the frequency-wavenumber domain as follows:

$$P_{z+\Delta z}\left(\omega,\mathbf{k_m},\mathbf{k_h}\right) = P_z\left(\omega,\mathbf{k_m},\mathbf{k_h}\right) e^{ik_z\Delta z}. \tag{2}$$

The vertical wavenumber performs the downward continuation on the concept of survey sinking. After each depth propagation step, the propagated wavefield is equivalent to the data that would have been recorded if all sources and receivers were placed at the new depth level (Schultz and Sherwood, 1980). The wavefields are propagated with two different velocities. A P velocity for the downgoing wavefield and a S velocity for the upcoming wavefield. The basic downward continuation is performed by applying the Double Square Root (DSR) equation,

$$k_z\left(\omega,\mathbf{k_s},\mathbf{k_g}\right) = \mathrm{DSR}\left(\omega,\mathbf{k_s},\mathbf{k_g}\right) = -\sqrt{\frac{\omega^2}{v_p^2(\mathbf{s},z)} - \mathbf{k_s}^2} - \sqrt{\frac{\omega^2}{v_s^2(\mathbf{g},z)} - \mathbf{k_g}^2}, \tag{3}$$

or in midpoint-offset coordinates:

$$\mathrm{DSR}(\omega,\mathbf{k_m},\mathbf{k_h}) = -\sqrt{\frac{\omega^2}{v_p^2(\mathbf{s},z)} - \frac{1}{4}(\mathbf{k_m}-\mathbf{k_h})\cdot(\mathbf{k_m}-\mathbf{k_h})} - \sqrt{\frac{\omega^2}{v_s^2(\mathbf{g},z)} - \frac{1}{4}(\mathbf{k_m}+\mathbf{k_h})\cdot(\mathbf{k_m}+\mathbf{k_h})}. \tag{4}$$

The common-azimuth downward-continuation operator takes advantage of the reduced dimensionality of the data space, that results of using a common-azimuth resorting of the data. Rosales and Biondi (2004) discuss how to do this resorting for converted waves data. The general continuation operator can then be expressed as follows (Biondi and Palacharla, 1996):

$$\begin{aligned} P_{z+\Delta z}\left(\omega,\mathbf{k_m},k_{x_h},y_h=0\right) &= \int_{-\infty}^{+\infty} dk_{y_h}\, P_z\left(\omega,\mathbf{k_m},k_{x_h},y_h=0\right) e^{-ik_z\Delta z} \\ &\approx P_z\left(\omega,\mathbf{k_m},k_{x_h},y_h=0\right) A\left(\omega,\mathbf{k_m},k_{x_h}\right) e^{-i\widehat{k_z}\Delta z}, \end{aligned} \tag{5}$$

since common-azimuth data is independent of $k_{y_h}$, the integral can be pulled inside and analytically approximated by the stationary phase method (Bleinstein, 1984). The application of the stationary phase method is based on a high-frequency approximation: that is, it assures that $\omega$ tends to infinity. By geometrical meanings we derive the stationary path approximation for converted waves.

The expression for $\widehat{k_z}$ comes from substituting the "stationary path" approximation into the expression for the full DSR of equation (4):

$$\widehat{k_z} = \mathrm{DSR}\left[\omega,\mathbf{k_m},k_{h_x},\widehat{k}_{h_y}(z),z\right] \tag{6}$$

where,

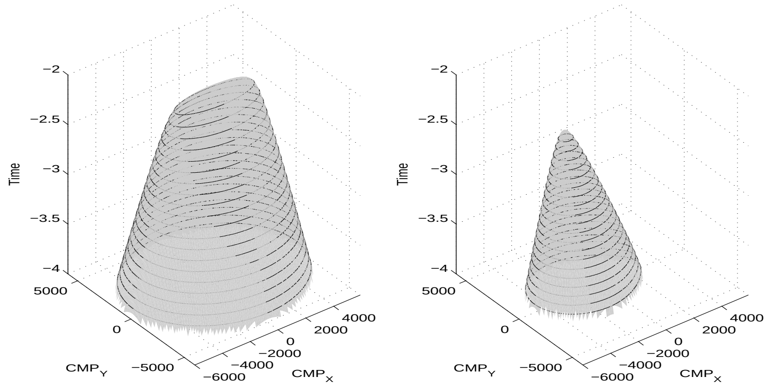


Figure 1: Summation surfaces for a constant media of P velocity equals 3000 m/s, and S velocity equals 1500 m/s and an offset of 2 km.

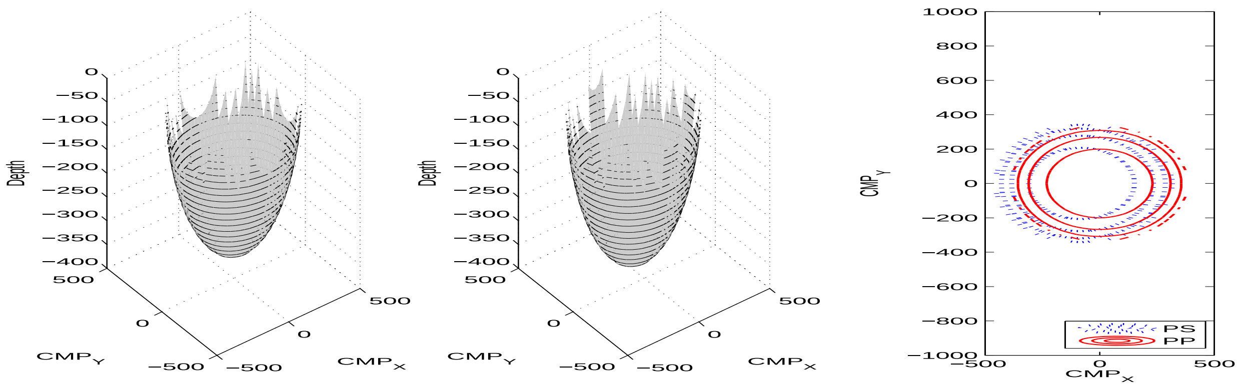


Figure 2: Spreading surfaces for an impulse at 0.480 s PP traveltime and 0.320 s PS traveltime, an offset of 200m, and assuming constant both P velocity of 2500 m and S velocity 1250 m. Right panel shows the contour lines comparison for both spreading surfaces.

$$\widehat{k}_{h_y}(z) = k_{ym} \frac{\sqrt{\frac{\omega^2}{v_s^2(\mathbf{g},z)} - \frac{1}{4}(k_{xm}+k_{xh})^2} - \sqrt{\frac{\omega^2}{v_p^2(\mathbf{s},z)} - \frac{1}{4}(k_{xm}-k_{xh})^2}}{\sqrt{\frac{\omega^2}{v_s^2(\mathbf{g},z)} - \frac{1}{4}(k_{xm}+k_{xh})^2} + \sqrt{\frac{\omega^2}{v_p^2(\mathbf{s},z)} - \frac{1}{4}(k_{xm}-k_{xh})^2}}. \tag{7}$$

## 4 Impulse response

Figure 1 presents the summation surfaces [equation (1)] for an impulse response at a depth of 500 m, a P velocity of 3000 m/s, an S velocity of 1500 m/s, and an in-line offset of 3000 m. The right panel shows the single mode PP summation surface and the left panel shows the converted mode PS summation surface. Similarly, Figure 2 shows the spreading surfaces; that is, the theoretical solution for depth on equation (1), the right panel presents the single mode PP spreading surface, the center panel shows the converted mode PS spreading surface, and the left panel compares the contour lines for both spreading surfaces.

Figure 3 shows the common azimuth impulse response for a constant P velocity of 2500 m/s and a constant S velocity of 1250 m/s, and a in-line offset of 200 m. The right panel exhibits the response for the single mode PP common azimuth migration operator, and the left panel exhibits the response for the converted mode PS migration operator.

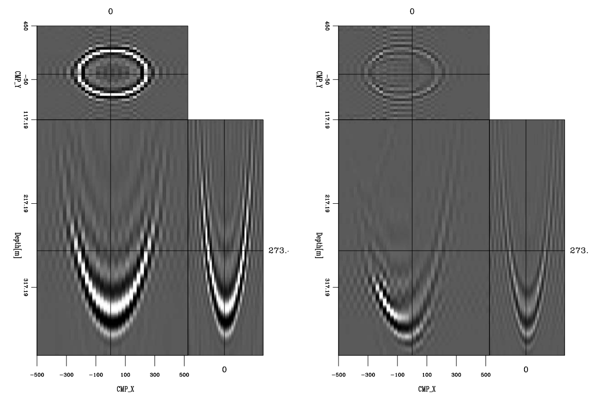

Figure 3: Impulse response for a point diffractor at 0.320 s PP traveltime and 0.480 s PS traveltime and constant velocity media of P velocity equals 2500 m/s and S velocity of 1250 m/s. Right panel presents the single mode PP, and the left panel presents the converted mode PS.

## 5 Conclusions

We present the converted mode PS 3-D common azimuth migration operator, the difference with this operator with respect to the single mode PP operator is the use of two different velocity fields; therefore, a more careful implementation is needed with references to the correct velocity model. We demonstrate that the subsurface area covered by PS common azimuth migration operator is different than the PP common azimuth migration operator; therefore, it is just the area that the two surfaces share the one to use for rock properties analysis based on the two complementary images. This might have important impacts on the characterization process for the reservoir.

## 6 REFERENCES


Alfaraj, M., 1992, Transformation to zero offset for mode converted waves by Fourier transform: 62nd Annual Internat. Mtg., Society Of Exploration Geophysicists, Expanded Abstracts, 974–977.

Biondi, B., and Palacharla, G., 1996, 3-D prestack migration of common-azimuth data: Geophysics, **61**, 1822–1832.

Bleinstein, N., 1984, Mathematical methods for wave phenomena: Academic Press.

Claerbout, J. F., 1985, Imaging the earth's interior: Blackwell Scientific Publications.

Harrison, M. P., and Stewart, R. R., 1993, Poststack migration of P-SV seismic data: Geophysics, **58**, no. 8, 1127–1135.

Huub Den Rooijen, P. G. M., 1991, Stacking of P-SV seismic reflection data using dip moveout: Geophysical Prospecting, **39**, no. 4, 585–598.

Iverson, W. P., Fahmy, B. A., and Smithson, S. B., 1989, VpVs from mode-converted P-SV reflections: Geophysics, **54**, no. 7, 843–852.

Rosales, D. A., and Biondi, B., 2004, Acquisition geometry regularization for multicomponent data: 74rd Annual Internat. Mtg., Society Of Exploration Geophysicists, Expanded Abstracts, 1162–1165.

Schultz, P. S., and Sherwood, J. W. C., 1980, Depth migration before stack: Geophysics, **45**, 376–393.

Tessmer, G., and Behle, A., 1988, Common reflection point data-stacking technique for converted waves: Geophysical Prospecting, **36**, no. 5, 671–688.